Provisional chapter

Atomization of Bio-Fossil Fuel Blends

Mansour Al Qubeissi, Nawar Al-Esawi and
Ruslana Kolodnytska

Additional information is available at the end of the chapter

Abstract

The importance of modeling multi-component fuel atomization, heating and evaporation has been recognized in many studies. The predictions of these models are crucial to the design and performance of combustion engines. Accurate modeling is essential to the understanding of these processes and ultimately to improving engine sustainability and reducing emission. The interest in bio-fossil fuel blends has been mainly stimulated by depletion of fossil fuels and the need to reduce carbon dioxide emissions that contribute towards climate change. This work presents a review of recent investigations into the heating and evaporation of multi-component blended fuel droplets in real internal combustion engine (ICE) conditions. The models consider the contribution of all groups of hydrocarbons in fossil (gasoline, diesel) fuels, methyl esters in 22 biodiesel fuels, and ethanol fuel. Diffusion of these fuel species, temperature gradient, and recirculation within droplets are accounted for. One important finding is that some fuel blends, for example B5 (5% biodiesel fuel and 95% diesel fuel) and E5 (5% ethanol fuel and 95% gasoline fuel), can give almost identical droplet lifetimes to the ones predicted for pure diesel and gasoline fuels; i.e. such mixtures can be directly used in conventional engines without modification.

Keywords: atomization, biodiesel, diesel, ethanol, fuel blends, gasoline, multi-component

1. Introduction

Biodiesel and ethanol fuels have been of great interest to scientists and public as biofuel resources of energy due to depletion of fossil fuels and impact on global warming [1, 2]. Also, compared to fossil fuel, biodiesel fuel has several advantages: it has less carbon dioxide emissions, higher flash point, higher lubricity and it is cost effective. In addition, diesel fuel can be blended with up to 20% of many biodiesel fuel types and directly injected in

standard diesel engines with minor tuning or no modification requirement in the ICE processes [3, 4]. According to Tier I and Tier II standards of the U.S.A. Environmental Protection Agency (EPA) (see [5] for details), biodiesel fuels produced within the last decade meet the minimum requirements of health risk [6]. Similarly, ethanol (or bio-ethanol) is commonly used as an alternative source of energy in the form of pure, or gasoline-blended, fuel in sparkling ignition (Otto cycle) engines [7]. Bioethanol is a very promising reactant for petrol engines and for biodiesel production industry, compared to methanol and fossil fuels. Lipids, such as fats or oils, react with ethanol to produce biodiesel. Also, it is renewable, green, and not toxic [8].

The delay in processes preceding the onset of combustion (mainly the spray formulation, and heating and evaporation of fuel droplets) in the internal combustion engines is crucial to the design and performance of these engines [9, 10]. The complexity of modeling evaporation processes should be taken into account as it involves detailed physics of heat transfer, mass transfer and fluid dynamics associated processes. Most of the studies on fuel droplet heating and evaporation analyses have been either based on considering individual components, described as 'discrete component' (DC) approach [11, 12], or on a probabilistic analysis of large numbers of hydrocarbons, described as 'continuous thermodynamics' [13–16] and 'distillation curve' [16–18] approaches. The DC approach is highly accurate and computationally efficient in the cases when a small number of hydrocarbons need to be taken into account. In the second approach, several simplifying assumptions are made; such as the assumption that hydrocarbon species inside droplets are mixed infinitely quickly, described as 'infinite diffusivity' approach, or they are not mixed at all, described as 'single component' approach.

The DC model, based on the analytical solutions to the equations of heat and mass transfer and species diffusion [19], has been verified against numerical simulations and validated against experimental data in [20] (see [9, 21] for more details). Following [22–25], the droplets heating and evaporation processes are analyzed by application of several blends of diesel-biodiesel fuels and ethanol-gasoline fuels.

The DC model is used for this analysis and applied to a broad range of diesel-biodiesel fuel fractions and ethanol-gasoline fractions. The mixture of EU diesel fuel with 22 types of widely used fatty acid methyl ester (FAME) biodiesel fuels have been investigated. These are: tallow (TME), lard (LME), butter (BME), coconut (CME), palm kernel (PMK), palm (PME), safflower (SFE), peanut (PTE), cottonseed (CSE), corn (CNE), sunflower (SNE), soybean (SME), rapeseed (RME), linseed (LNE), tung (TGE), hemp-oil, produced from hemp seed oil in the Ukraine (HME1), hemp-oil, produced in European Union (HME2), canola (CAN), waste cooking-oil (WCO), yellow grease oil (YME), camelina (CML), and jatropha (JME). Droplets with four fractions of diesel-biodiesel blends have been investigated in the DC model. These are 5% biodiesel with 95% diesel fuels (B5), 20% biodiesel with 80% diesel fuels (B20), 50% biodiesel with 50% diesel fuels (B50), pure biodiesel (B100) and pure diesel fuels (PD). For the ethanol-gasoline blends, droplets with five fractions have been investigated in the DC model. These are 5% ethanol with 95% gasoline fuels (E5), 20% ethanol with 80% gasoline fuels (E20),

50% ethanol with 50% gasoline fuels (E50), 85% ethanol with 15% gasoline fuels (E85), pure ethanol (E100) and pure gasoline fuels (E0).

In this work, the discrete component model is utilized to analyze the droplets heating and evaporation of diesel-biodiesel and ethanol-gasoline fuel blends.

2. Model

The diesel-biodiesel blends are represented by a mixture of 22 types of biodiesel fuels with up to 22 species of methyl ester and diesel fuel, formed of 98 hydrocarbons represented by 9 groups (see [26] for more details). The ethanol-gasoline blends are represented by a mixture of ethanol and fuel used in advanced combustion engines, type C (FACE C) gasoline fuel, formed of 20 hydrocarbons, in 6 groups categorized according to their chemical structures and thermodynamic and transport properties (see [27] for more details). The thermodynamic and transport properties of diesel are inferred from [28], and those of biodiesel fuel are inferred from [26, 29] respectively; while properties of ethanol and gasoline fuel are taken from [27, 30] respectively. The contribution of species and average droplet temperatures are taken into account in the calculation of all fuel properties. All units used in our analyses are SI unless indicated otherwise.

2.1. Spray model

Two parameters for the modeling of droplet breakup based on liquid properties have been introduced by Eggers [31]; these are time and length parameters. For the calculation of length parameter (LP), we take into account viscosity, density and surface tension of liquid, as:

$$\mathrm{LP} = \frac{\nu_f^2 \rho_f}{\sigma} \tag{1}$$

We have proposed to use LP for spray parameters calculation including Sauter mean diameter (SMD) and spray penetration [32, 33]. Our analysis shows that the spray penetration of biodiesels will be proportional to $\mathrm{LP}^{0.1}$:

$$S_{tip} = A_{LP}\left(d_0^{0.5}\, p_{inj}^{0.36}\, \rho_g^{-0.29}\right) \mathrm{LP}^{0.1}\, t_{inj}^{0.5} \tag{2}$$

where d_0 is nozzle diameter, ρ_g is gas density, and p_{inj} is injection pressure.

It has been suggested in [34] that the better prediction of SMD for diesel and biodiesel fuels can be predicted as:

$$\mathrm{SMD} = 3.08\, \nu_f^{0.385} \left(\sigma \rho_f\right)^{0.737} \rho_g^{0.06}\, \Delta p^{-0.54} \tag{3}$$

We have used the following expression to calculate the middle droplet diameter of biodiesel fuels:

$$\mathrm{SMD} = 23\, d_0^{0.35}\, \mathrm{LP}^{0.1}\, \Delta p^{-0.54}\, \rho_g^{0.06} \tag{4}$$

where Δp is the pressure difference.

For ethanol-kerosene blends for air-blast atomizer, it was found that the SMD can be calculated as [33]:

$$\mathrm{SMD} = 2253\, \mu_l^{0.633}\, p_l^{-0.507}\, p_a^{-4.565\times10^{-3}} \tag{5}$$

2.2. Evaporation model

The DC model is based on the analytical solutions to the heat transfer and species diffusion equations via the effective thermal conductivity (ETC) model and effective diffusivity (ED) model. The importance of these models can be attributed to the fact that they take into account the recirculation, temperature gradients and species diffusion inside droplets. The heat conduction equation for the temperature $T = T(t, R)$ in the liquid phase in a spherical droplet can be presented as:

$$\frac{\partial T}{\partial t} = \kappa_{\mathrm{eff}}\left(\frac{\partial^2 T}{\partial R^2} + \frac{2}{R}\frac{\partial T}{\partial R}\right) \tag{6}$$

where, t is the time, R is the distance from the center of the droplet, T is the temperature and κ_{eff} is the effective thermal diffusivity.

The time evolution of species mass fractions at any R is described by the following Eq. [19, 35]:

$$\frac{\partial Y_{li}}{\partial t} = D_{\mathrm{eff}}\left(\frac{\partial^2 Y_{li}}{\partial R^2} + \frac{2}{R}\frac{\partial Y_{li}}{\partial R}\right) \tag{7}$$

where, $i > 1$, D_{eff} is the effective liquid species diffusivity, $D_{\mathrm{eff}} = \chi_Y D_l$, D_l is the liquid diffusivity and χ_Y is a coefficient that varies between 1 and 2.72 [19, 20]. χ_Y takes into account the recirculation inside droplets.

3. Fuel compositions

The commercial diesel fuel selected in the present work conforms to standard European Union fuel (EN590), formed of 98 hydrocarbons represented by 9 groups, categorized according to their chemical formulae. Molar fractions of various components in this fuel are presented in **Table 1**, inferred from [28].

For gasoline fuel, the number of the components with identical chemical formulae and close thermodynamic and transport properties are replaced with characteristic components leading to reducing the original composition of gasoline fuel (83 components) to 20 components only, represented by 6 hydrocarbon groups as presented in **Table 2** (see [27] for more details). The biodiesel fuels are formed of up to 22 species of fatty acid methyl ester (FAME). These are inferred from [24, 36] and presented in **Table 3**.

Carbon no	N-Alkane	Iso-alkane	Cycloalkane	Bi-cycloalkane	Tri-cycloalkane	Alkylbenzene	Indane & tetraline	Naphthalene	Diaromatic	Phenanthrene
C8	0.308	—	—	—	—	0.497	—	—	—	—
C9	1.0513	1.9807	—	—	—	3.2357	—	—	—	—
C10	1.2635	3.7906	0.6408	0.6926	—	5.3584	1.3157	1.9366	—	—
C11	1.1002	2.0628	1.8745	1.0524	—	0.9492	1.3632	2.5290	—	—
C12	0.9866	1.6290	1.6951	0.9753	—	1.9149	1.1951	1.4012	—	—
C13	0.9646	1.5793	1.2646	0.6611	—	0.6873	1.0652	0.7692	0.3834	—
C14	1.0146	1.6351	1.3633	0.5631	0.0914	0.6469	0.8406	0.4879	0.3217	0.0768
C15	1.2051	1.9595	1.2353	0.4314	0.1799	0.4782	0.7051	0.3843	0.2589	0.2033
C16	1.0442	1.6137	1.0449	0.4921	0.1773	0.4564	0.6684	0.2854	0.2602	0.1705
C17	1.0564	1.8041	1.0162	0.6529	0.4001	0.4204	0.5598	0.2072	—	0.1154
C18	1.0596	2.1807	1.2848	0.6554	0.3304	0.5234	0.5357	0.2358	—	0.0917
C19	1.0916	2.438	1.3566	0.9901	0.2159	0.3226	0.3403	0.2151	—	—
C20	0.7054	1.5284	0.9961	0.1965	0.1696	0.2848	0.3227	0.2256	—	—
C21	0.3756	1.0674	0.5374	0.0935	—	0.2032	0.1638	—	—	—
C22	0.2328	0.5662	0.304	0.0701	—	0.0969	0.0781	—	—	—
C23	0.1083	0.2889	0.109	0.0488	—	0.0494	—	—	—	—
C24	0.0461	0.1442	0.0755	0.0234	—	0.0473	—	—	—	—
C25	0.0221	0.0776	0.0445	0.0169	—	—	—	—	—	—
C26	0.0106	0.0319	0.0214	—	—	—	—	—	—	—
C27	0.0052	0.0257	0.0155	—	—	—	—	—	—	—
Total%	13.65	26.40	14.88	7.62	1.56	16.17	9.15	8.68	1.22	0.66

Table 1. The diesel fuel composition (molar fractions) used in our analyses [28].

m	Group	Molar fractions (%)	Number of components
1	N-Alkanes	28.50	5
2	Iso-alkanes	65.18	8
3	Aromatics	4.40	4
4	Indanes/naphthalenes	0.10	1
5	Cycloalkanes	0.33	1
6	Olefins	1.49	1

Table 2. The groups of gasoline fuel molecules, their molar fractions, and the numbers of components within each group, as used in our models [27].

FAME	Biodiesel fuels										
	TME	LME	BME	CME	PMK	PME	SFE	PTE	CSE	CNE	SNE
C8:0	—	—	5.2	6.0	2.6	—	—	—	—	—	—
C10:0	—	—	2.8	8.0	4.0	—	—	—	—	—	—
C12:0	0.2	—	3.4	50.0	50.0	0.3	—	—	—	—	—
C14:0	2.5	1.0	11.0	15.0	17.0	1.3	—	0.5	2.0	1.0	—
C15:0	—	—	—	—	—	—	—	—	—	—	—
C16:0	27.9	26.0	31.7	9.0	8.0	45.1	5.2	8.0	19.0	9.0	5.9
C17:0	—	—	—	—	—	—	—	—	—	—	—
C18:0	23.0	14.0	10.8	3.0	1.7	4.5	2.2	4.0	2.0	2.5	4.2
C20:0	0.4	—	0.4	—	1.5	0.4	—	7.0	—	—	1.4
C22:0	0.4	—	0.4	—	1.5	0.2	—	7.0	—	—	1.4
C24:0	—	—	—	—	—	—	—	—	—	—	—
C16:1	2.5	2.8	2.4	—	0.4	0.2	—	1.5	—	1.5	—
C17:1	—	—	—	—	—	—	—	—	—	—	—
C18:1	40.0	44.0	26.3	7.0	12.0	38.4	76.4	49.0	31.0	40.0	18.5
C20:1	0.3	2.0	1.0	—	—	—	—	—	2.5	1.0	—
C22:1	0.3	2.0	1.0	—	—	—	—	—	2.5	1.0	—
C24:1	—	—	—	—	—	—	—	—	—	—	—
C18:2	2.0	8.0	3.0	2.0	1.3	9.2	16.2	23.0	41.0	44.0	68.3
C20:2	—	—	—	—	—	—	—	—	—	—	—
C18:3	—	—	0.6	—	—	0.2	—	—	—	—	0.3
C20:3	—	—	—	—	—	—	—	—	—	—	—
C18:4	—	—	—	—	—	—	—	—	—	—	—
Others	0.5	0.2	—	—	—	0.2	—	—	—	—	—

FAME	Biodiesel fuels										
	TGE	HM1	SME	LNE	HM2	CAN	WCO	RME	CML	JTR	YGR
C8:0	—	—	—	—	—	—	—	—	—	—	—
C10:0	—	—	—	—	—	—	—	—	—	—	—
C12:0	—	—	—	—	—	—	0.2	—	0.4	0.1	0.2
C14:0	—	—	0.3	0.2	—	—	0.7	—	2.6	0.3	0.8
C15:0	—	—	—	—	—	—	—	—	—	—	0.1
C16:0	3.6	6.6	10.9	6.2	6.5	4.5	15.7	4.9	5.8	14.3	16.0
C17:0	—	0.2	—	—	—	0.1	0.2	—	—	0.1	0.1
C18:0	2.6	2.1	4.4	0.6	2.5	2.0	6.1	1.7	2.7	5.9	6.9
C20:0	—	0.5	0.4	—	0.9	0.6	0.4	0.6	1.3	0.2	0.3
C22:0	13.1	0.3	—	—	—	0.4	0.4	—	0.9	0.2	0.4
C24:0	—	0.2	—	—	—	0.2	0.3	—	0.7	2.5	0.2
C16:1	—	0.3	—	—	—	0.4	0.7	—	—	1.0	0.9
C17:1	—	—	—	—	—	—	—	—	—	—	0.1
C18:1	10.1	11.9	24.0	18.0	11.9	59.7	42.8	26.6	15.9	38.9	43.2
C20:1	0.8	0.3	—	—	0.9	1.5	0.6	—	13.7	0.1	0.5
C22:1	—	0.2	—	—	—	0.4	0.2	22.3	2.9	0.1	0.1
C24:1	—	0.2	—	—	—	—	—	0.8	0.2	0.1	4.3
C18:2	13.8	56.6	52.8	16.0	54.7	20.8	29.4	24.8	16.0	34.8	24.3
C20:2	—	—	—	—	—	—	—	—	1.4	—	—
C18:3	51.6	20.6	7.2	59.0	20.1	9.4	2.0	9.7	33.8	0.3	1.1
C20:3	—	—	—	—	—	—	—	—	0.8	—	—
C18:4	—	—	—	—	—	—	—	—	—	—	0.5
Others	4.4	—	—	—	2.5	—	0.3	8.6	0.9	1.1	—

Table 3. Biodiesel fuel compositions [24, 36].

4. Results

4.1. Atomization

The importance of spray breakup associated phenomena for various applications is well recognized and has been extensively investigated experimentally and numerically by engineers, environmentalists, automotive industrialists, pharmaceutics, and agriculturists [21, 37–41]. A rigorous representation of spray breakup is very complicated procedure as it would involve accurate estimation of nozzle flow, initial formation of ligaments, instabilities, cavitation, and droplets associated physics and their subsequent breakup, heating, evaporation, the entrainment of air and the effects of turbulence [21, 40]. The efficiency of the combustion process and emission reduction in internal combustion engines depends on the atomization characteristics;

the most important characteristics of which are droplet Sauter mean diameter (SMD), cone angle, droplet size distributions. The SMD of biodiesel and diesel fuel droplets at temperature 80°C, as reported in [34], are shown in **Table 4**.

Reference	PME	HME1	HME2	RME	SME	Diesel
Eq. (3)	25.1	—	—	28.8	25.7	17.7
Eq. (4)	—	23.55	23.55	26.69	23.87	18.3

Table 4. The SMDs (in μm) of typical biodiesel and diesel fuel droplets at 80°C.

The average value of biodiesel fuel droplet SMDs (25.32 μm) is larger than those of diesel fuel droplets, which can be attributed to the higher viscosity of biodiesel fuels [34].

4.2. Probability density function for biodiesel spray

It is very important to know how biofuel droplets distribute/spread by size after the atomization. **Figure 1** shows the drop-size probability density for diesel and biodiesel fuels when experimental data [42] are fitted by maximum entropy method [43].

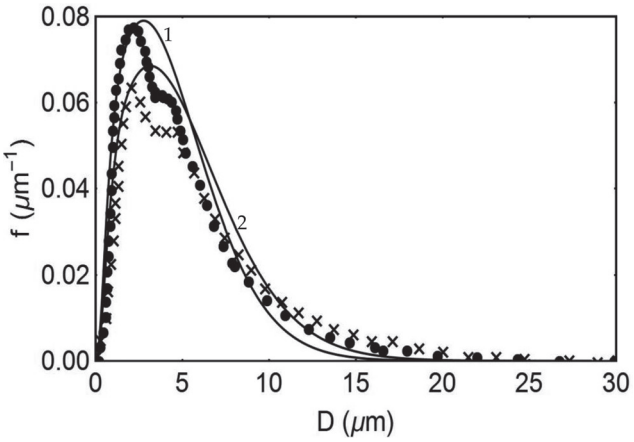

Figure 1. Probability density functions of the droplet diameters at distance of 15 mm from nozzle exit [43]; 1- for diesel fuel, 2 - for biodiesel fuel. Experimental data for diesel (•) and biodiesel (×) fuels are inferred from [43, 44].

The case shown in **Figure 1** is close to realistic diesel engine conditions with an injection pressure of 100 MPa. In this case, diesel fuel has emerged from the nozzle orifice with a velocity of about 100 m/s as ultra-high-speed videos shown in [40]. We assumed that biodiesel has a lower mean injection velocity than diesel, but this difference is compensated by the higher value of middle droplet diameters for biodiesel.

4.3. Blended diesel-biodiesel fuel droplets

The DC model is facilitated for the analysis of heating and evaporation of diesel-biodiesel fuel droplets of initial radius R_{d0} = 12.66 μm and temperature T_0 = 360 K. The droplets are moving at U_d = 10 ms^{-1} in still air of pressure and temperature equal to p_g = 30 bar and T_g = 800 K, respectively. The evolutions of droplet surface temperatures (T_s) and radii (R_d) for three mixtures of diesel-biodiesel fuels (B5, B20, B50) and pure biodiesel fuel (B100) of 22 types of biodiesel fuels are analyzed. Typical examples of these results are presented in **Figures 2–7**.

In **Figures 2–7** (some examples of the analyzed blends of diesel-biodiesel fuels), one can see that increasing the concentration of biodiesel from B5 to B100 has a noticeable effect on the evolution of R_d and T_s. In addition, the predicted surface temperature of the droplet for B100 is higher than that of B5 during the initial heating period. According to [22], the droplet break-up process can be enhanced as a result of the increase in droplet surface temperature. This can be attributed to the decrease in droplet surface tension. A full illustration of the results provided in **Figures 2–7** are shown in **Table 5**. The droplet lifetimes of 22 types of biodiesel fuel mixtures with PD fuel and their differences from the one predicted for PD fuel (2.25 ms) are presented in this table.

As can be seen from **Table 5**, the droplet lifetime for B100 of RME fuel is 6% less than that of PD. This reduction does not exceed 0.4% for the B5 fuel blend for the same fuel. Also, droplet lifetime of TGE biodiesel fuel droplet is noticeably close to that of PD droplet; it is less than 8 and 0.5% for B100 and B5 mixtures, respectively. The maximum difference in droplet lifetimes for these fuels is up to 21.6% (B100 CME), which cannot be sacrificed in any engineering application, and it is always higher than 5.29% (RME) compared to PD, which may be tolerated in some limited engineering applications.

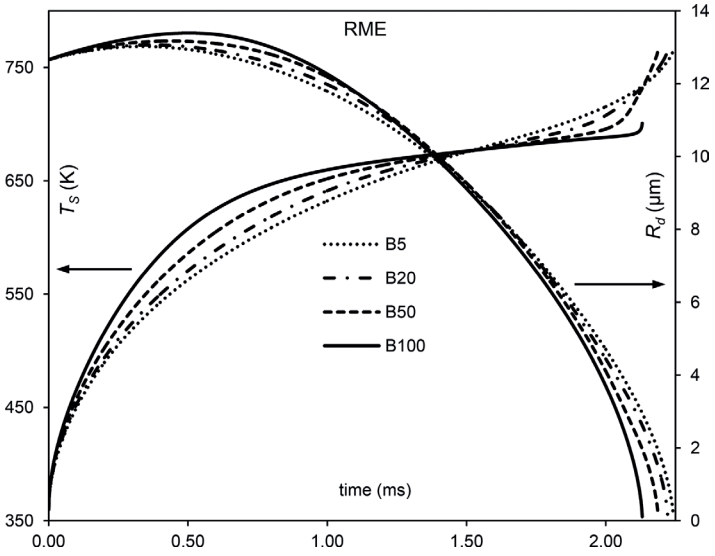

Figure 2. Droplet surface temperatures T_s and radii R_d versus time for four fractions of diesel-RME biodiesel fuels: B5, B20, B50 and B100.

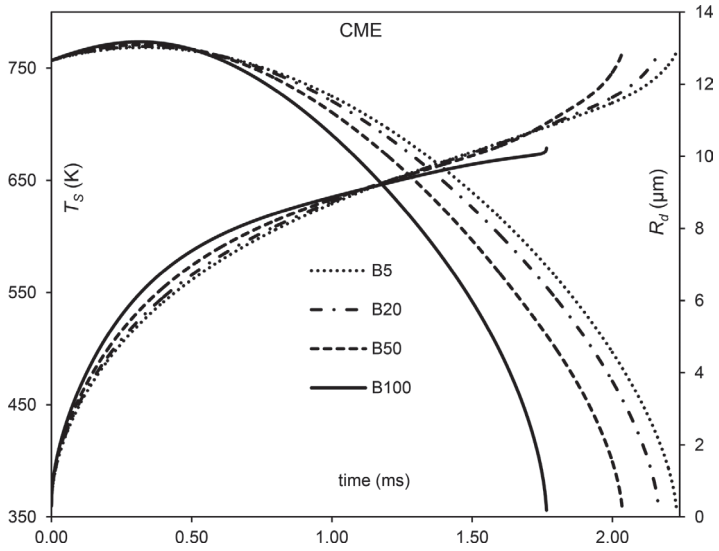

Figure 3. Droplet surface temperatures T_s and radii R_d versus time for four fractions of diesel-CME biodiesel fuels: B5, B20, B50 and B100.

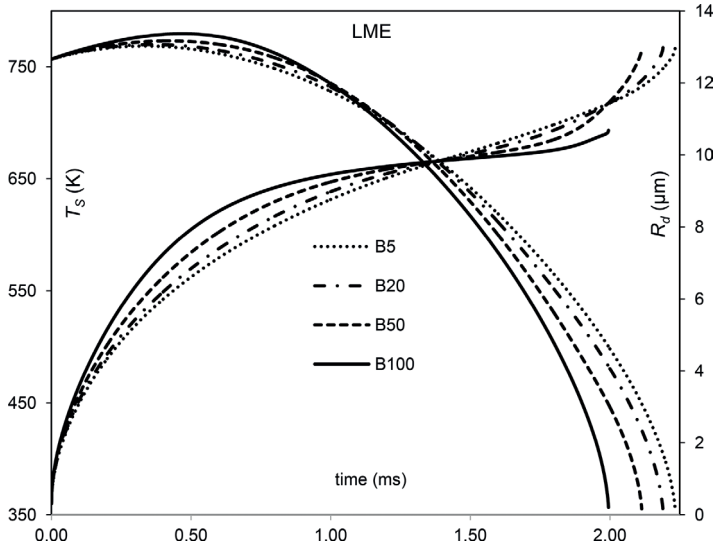

Figure 4. Droplet surface temperatures T_s and radii R_d versus time for four fractions of diesel-LME biodiesel fuels: B5, B20, B50 and B100.

In some previous studies (for example, see [22, 23]) the heating and evaporation of PD fuel droplets and their comparison to the results of diesel-biodiesel blends were analyzed. For instance, in [23] the droplet lifetime for B100 of WCO was shown to be 11% less than that of PD. While in [22], the droplet lifetime for B100 of SME fuel was shown to be 6% less than that

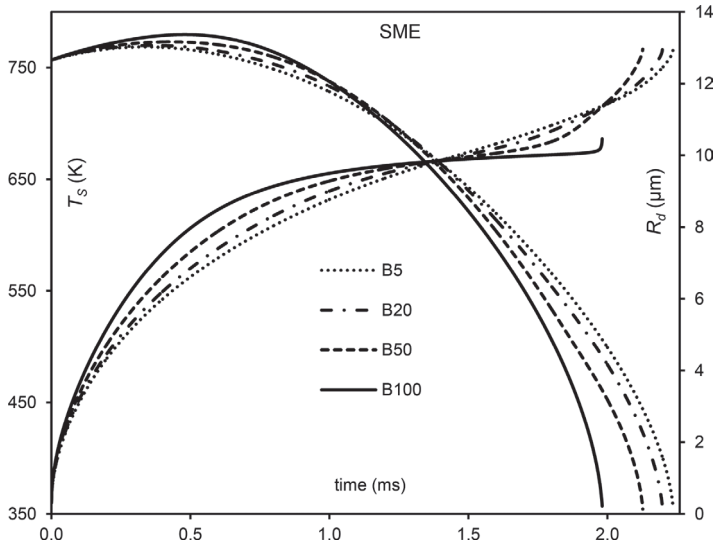

Figure 5. Droplet surface temperatures T_s and radii R_d versus time for four fractions of diesel-SME biodiesel fuels: B5, B20, B50 and B100.

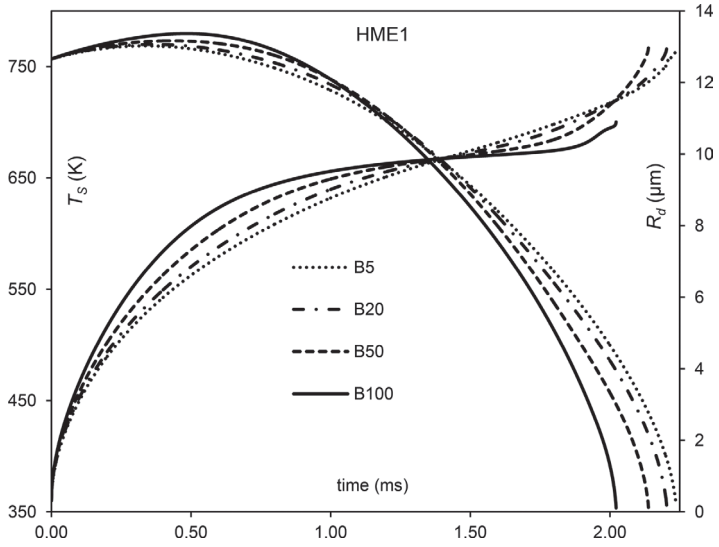

Figure 6. Droplet surface temperatures T_s and radii R_d versus time for four fractions of diesel-HME1 biodiesel fuels: B5, B20, B50 and B100.

for PD. In this study, similar trends were predicted for the same fuels. This prediction, however, was different for the other types of biodiesel fuel presented in this work. For example, the B100 droplet lifetimes for CME and PMK biodiesel fuels showed deviations of 21.6 and 18%, respectively, from that of PD fuel.

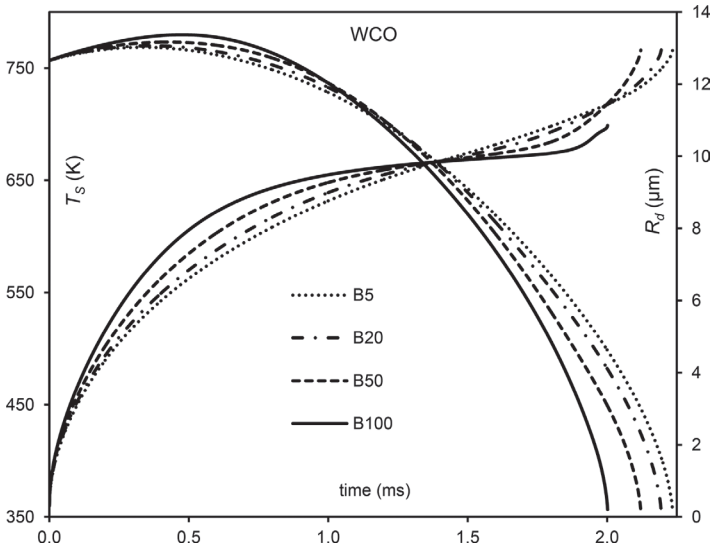

Figure 7. Droplet surface temperatures T_s and radii R_d versus time for four fractions of diesel-WCO biodiesel fuels: B5, B20, B50 and B100.

A general trend shows that droplets' lifetimes of all 22 types of B5 diesel-biodiesel blends that are used in this study deviate with less than 1% from the one predicated for PD droplets. This concludes the possibility of labeling diesel-biodiesel blends, with up to about 5% biodiesel concentration, without modifying the automotive system is achievable. For some fuel blends (for example B20 RME, TGE, LNE, and HME1), this deviation (up to 2%) is still relatively negligible to mix higher biodiesel concentrations (for example, 20% biodiesel and 80% diesel fuels) without losing the main feature of these processes (i.e. droplet lifetime).

The difference in thermodynamic and transport properties between hydrocarbons and methyl esters is the main reason for the influence of biodiesel fuel fractions on the heating and evaporation of diesel fuel droplets. For instance, when increasing the biodiesel fractions, the droplet surface temperature tends to reach a plateau during the evaporation process, which is similar to the case of single component model (see [20, 28]). Also, the significance of such behavior can change depending on the input parameters and ambient conditions.

A typical example of time evolutions of mass fractions at the surface of droplets (Y_{lis}) of selected nine species of B50 fuel mixture of diesel with RME is shown in **Figure 8**; in which, the curves 1, 2 and 3, refer to alkane hydrocarbons of $C_{27}H_{56}$, $C_{25}H_{52}$ and $C_{23}H_{48}$, respectively; and the curves 4, 5 and 6, refer to cycloalkane hydrocarbons of $C_{27}H_{54}$, $C_{25}H_{50}$ and $C_{23}H_{46}$, respectively; and the curves, 7 and 8, refer to rapeseed methyl esters of $C_{19}H_{36}O_2$ and $C_{19}H_{34}O_2$, respectively, under the same conditions used in **Figures 2–7**.

As can be seen from **Figure 8**, the diffusion of mass fractions of components at the surface of droplets is typical and similar to those presented in previous studies. The mass fractions of the heavy components, for example $C_{27}H_{56}$ (1) and $C_{27}H_{54}$ (4), increase with time at the

Biodiesel fuels	B100		B50		B20		B5	
	Lifetime (ms)	Diff. (%)	Lifetime (ms)	Diff. (%)	Lifetime (ms)	Diff. (%)	Lifetime (ms)	Diff. (%)
TME	1.967	12.6	2.102	6.6	2.184	2.9	2.232	0.80
LME	1.995	11.3	2.114	6.0	2.190	2.7	2.234	0.71
BME	1.943	13.6	2.089	7.2	2.180	3.1	2.232	0.80
CME	1.765	21.6	2.036	9.5	2.166	3.7	2.229	0.93
PMK	1.846	18.0	2.050	8.9	2.169	3.6	2.230	0.89
PME	1.944	13.6	2.097	6.8	2.183	3.0	2.232	0.80
SFE	1.980	12.0	2.122	5.7	2.195	2.4	2.235	0.67
PTE	2.052	8.8	2.138	5.0	2.199	2.3	2.236	0.62
CSE	2.014	10.5	2.128	5.4	2.197	2.4	2.236	0.62
CNE	2.002	11.0	2.128	5.4	2.197	2.4	2.236	0.62
SNE	2.011	10.6	2.132	5.2	2.200	2.2	2.237	0.58
SME	1.981	12.0	2.127	5.5	2.198	2.3	2.236	0.62
RME	2.131	5.3	2.188	2.8	2.222	1.2	2.242	0.36
LNE	1.991	11.5	2.141	4.8	2.206	2.0	2.239	0.49
TGE	2.085	7.3	2.160	4.0	2.211	1.7	2.240	0.44
HME1	2.022	10.1	2.138	5.0	2.203	2.1	2.237	0.58
HME2	1.994	11.4	2.135	5.1	2.202	2.1	2.238	0.53
CAN	2.014	10.5	2.130	5.3	2.199	2.3	2.236	0.62
WCO	2.002	11.0	2.121	5.7	2.194	2.5	2.235	0.67
CML	2.064	8.3	2.153	4.3	2.209	1.8	2.239	0.49
JTR	2.047	9.0	2.133	5.2	2.198	2.3	2.236	0.62
YGR	2.077	7.7	2.149	4.5	2.203	2.1	2.237	0.58

Table 5. Estimation of biodiesel fuel droplets lifetimes and their differences compared with those of PD fuel (2.25 ms), under the same conditions shown in **Figures 2–7**.

expense of the lighter ones leading to different properties of duel near the evaporation time. The impacts of ambient pressure on the estimated droplet lifetimes of various LME biodiesel-diesel mixtures are shown in **Figure 9**.

It can be seen from **Figure 9** that the impacts of increasing ambient pressure (20–60 bar) at a relatively high ambient temperature (800 K) on reducing the estimated droplet lifetimes are proportional with almost the same effect for all mixtures (B5 – B100), but with lower droplet lifetimes for B100 and higher ones for B5. One can see that the difference in droplet lifetimes for different blends increase with increasing ambient pressure. Typical ambient pressure at diesel injection time is about 32 bar, however, it can be concluded that minimizing the pressure to 32 bar is better for high blend ratios, as the less the pressure the less the expected deviation in droplet lifetimes.

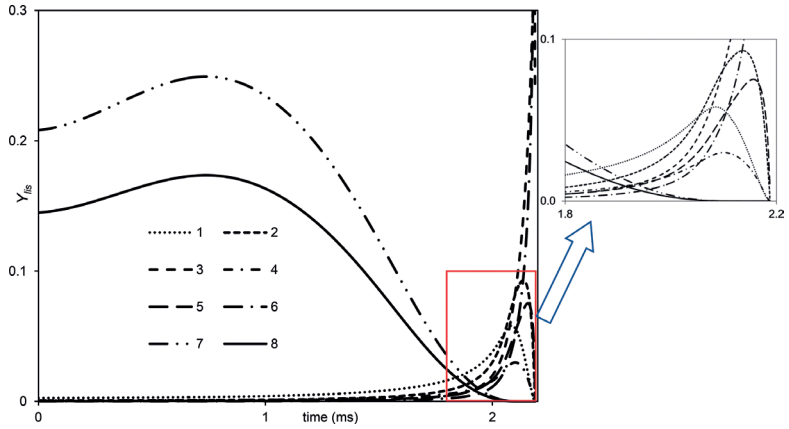

Figure 8. The liquid mass fractions at the surface of droplet (Y_{lis}) versus time for selected 8 components of 106 components of B50 (50% diesel hydrocarbons and 50% rapeseed methyl ester (RME)) fuel mixture.

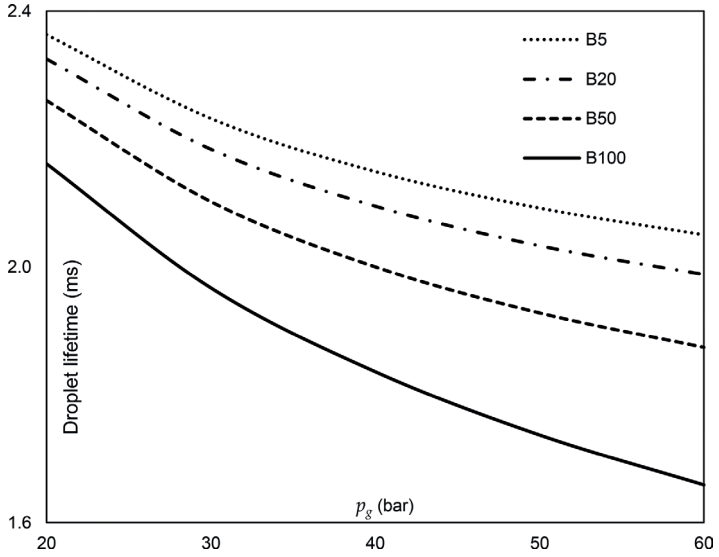

Figure 9. The effect of ambient pressure on diesel-biodiesel (LME) droplet lifetimes.

4.4. Blended ethanol-gasoline fuel droplets

The DC model is facilitated for the analysis of heating and evaporation of ethanol-gasoline fuel droplets of initial radius R_{d0} = 12μm and temperature T_0 = 296 K. The droplets are assumed to be moving at U_d = 24 ms^{-1} in still air of pressure and temperature equal to p_g = 9 bar and T_g = 545 K, respectively. The evolutions of droplet surface temperatures (T_s) and radii (R_d) for the ethanol-gasoline fuel mixtures are analyzed. The mixtures are: E0 (pure gasoline), E5 (5% ethanol, 95% gasoline), E20 (20% ethanol, 80% gasoline), E50 (50% ethanol, 50% gasoline), E85 (85% ethanol, 15% gasoline) and E100 (pure ethanol).

In **Figures 10–11**, the plots for droplet radii and transient surface temperatures are shown, respectively, for six mixing ratios of ethanol-gasoline fuel blends (E0 – E100).

In **Figure 10**, the droplet lifetime for pure gasoline fuel (E0) is the smallest. This increases with the increase of ethanol fraction from E0 to E100. The error in predicted droplet lifetime of E100 is

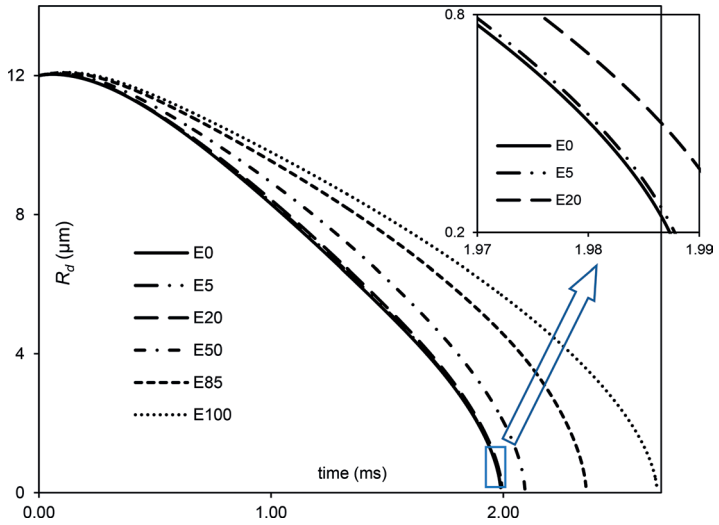

Figure 10. Droplet radii R_d versus time for six fractions of ethanol-gasoline fuels: E0, E5, E20, E50, E85 and E100.

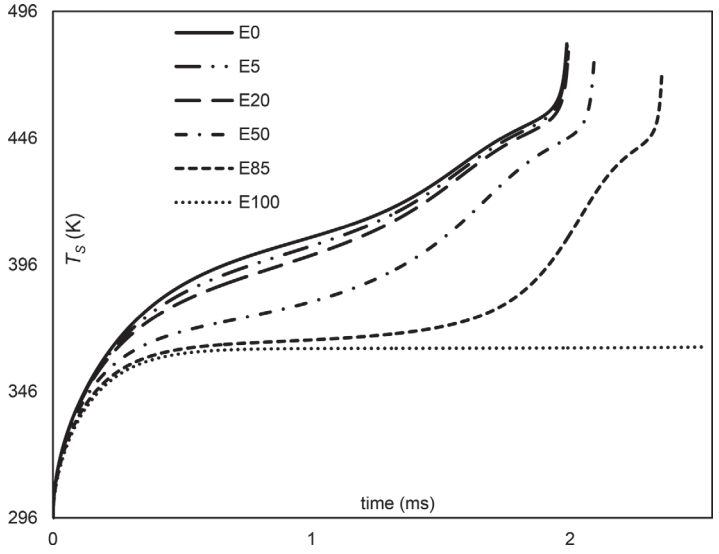

Figure 11. Droplet surface temperatures T_s versus time for six fractions of ethanol-gasoline fuels: E0, E5, E20, E50, E85 and E100.

Blends	Time (ms)	Diff%
E0	1.988	—
E5	1.989	0.050
E20	1.994	0.302
E50	2.093	5.282
E85	2.356	18.511
E100	2.662	33.903

Note:

$$\text{Diff }\% = \frac{\left|(tim\,e_{EN} - tim\,e_{E0})\right|}{tim\,e_{E0}} \times 100\%$$

Table 6. The impact of ethanol/gasoline fuel blends on the estimated droplet lifetimes.

33.9% compared to the one predicted for E0. In **Figure 11**, the impact of increasing the ethanol/gasoline fraction from E0 to E100 is seen to be significant. The deviation in the predicted droplet surface temperature for E100 is 24.3% compared to the one predicted for E0. The impacts of different ethanol/gasoline fuel mixtures on droplet lifetimes are presented in **Table 6**.

The droplet lifetimes of ethanol-gasoline fuel mixtures (**Figures 10–11**) have been estimated under standard engine conditions. The impact of different ambient conditions on these predictions is presented in **Figures 12** and **13**.

As can be seen from **Figures 12** and **13**, increasing the ambient temperature (500 to 650 K), or pressure (3 to 20 bar), leads to a proportional reduction in estimated droplet lifetimes with almost the same effect for all ethanol-gasoline blends.

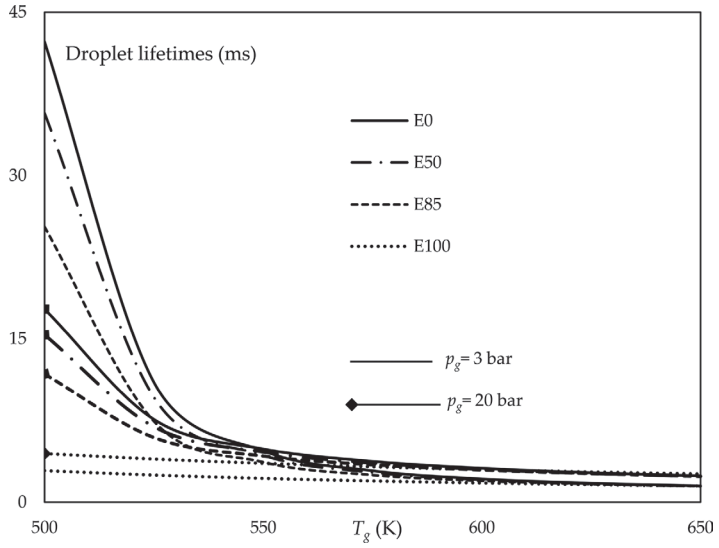

Figure 12. The impact of ambient temperatures on droplet lifetimes for E0, E50, E85 and E100 fuel blends, estimated at ambient pressures 3 and 20 bar.

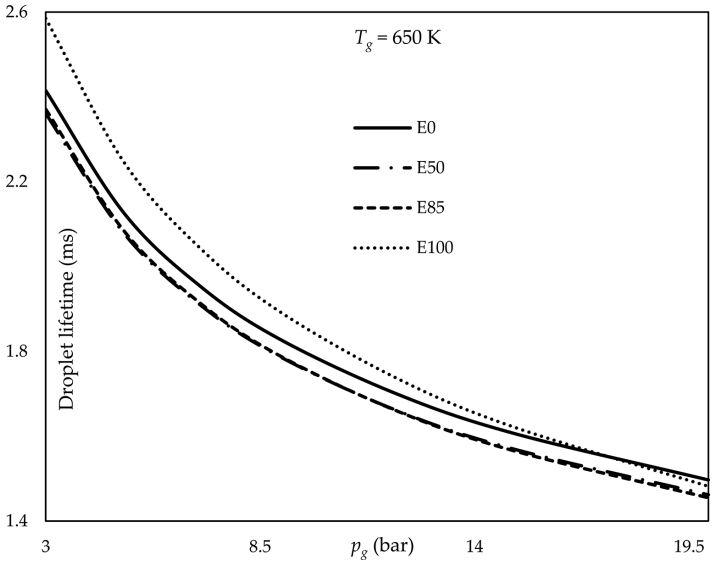

Figure 13. The impact of ambient pressures on droplet lifetimes for E0, E50, E85 and E100 fuel blends, estimated at ambient temperature 650 K.

5. Conclusion

In this chapter, the maximum entropy method was applied for the droplet distribution of diesel and biodiesel fuel sprays in conditions relevant to diesel internal combustion engines. The droplet distribution for biodiesel was more skewed to the right compared to the predicted diesel spray. The theoretical distribution indicated that biodiesel fuel droplets are larger than those of diesel fuel. The model was validated against available experimental data to show a reasonable agreement between both results.

The discrete component model was used to analyze the heating and evaporation of blended diesel-biodiesel fuel sprays and droplets using 22 types of biodiesel, European standard diesel, gasoline FACE C, and ethanol-gasoline fuels. The full compositions of diesel, biodiesel and gasoline fuels were considered. The diesel and gasoline fuels consisted of 98 and 20 hydrocarbons respectively, while the 22 biodiesel fuels consisted of 4 to 18 components of methyl esters.

The effect of increasing biodiesel fuel concentration on the evolutions of droplet surface temperatures and evaporation times was clearly illustrated. The predicted B5 fuel droplet lifetimes for the 22 types of biodiesel fuel were only 1% less than that of pure diesel (PD) fuel. The RME biodiesel fuel droplets were observed to have lifetimes close to that of PD fuel, where their predicted lifetimes for B5 and B100 droplets were up to 0.4 and 0.6%, respectively, less than the one estimated for PD fuel droplet. However, for ethanol, the predicted E5 fuel droplet lifetimes were only 0.05% greater than that of pure gasoline (E0) and only 0.3% greater for E20.

To conclude, the B5 fuel droplet lifetimes for all 22 types of biodiesel fuels used in this study are almost identical to the one predicted for PD fuel; i.e. diesel fuel can be possibly blended with up to 5% biodiesel fuel without any noticeable effect on the evolutions of their droplet radii or surface temperatures. Similarly, the E5 and E20 fuel droplet lifetimes are almost identical to the one predicted for E0 fuel; i.e. gasoline fuel can be possibly blended with up to 20% ethanol fuel without/minimal modifications to the gasoline engine. Also, increasing the ambient pressure, or temperature, will lead to a faster evaporation of E0-E100 droplets regardless of their blending ratios.

Acknowledgements

The authors are grateful to the British Council (ERASMUS+ Programme, EU Commission grant, award No. 2016-2-UK01-KA107-034987) and the Centre for Mobility and Transport – Coventry University for providing financial support to work on this project.

Nomenclature

B#	#% biodiesel/diesel fraction
BME	butter methyl ester
CAN	canola methyl ester
CME	coconut methyl ester
CML	camelina methyl ester
CNE	corn methyl ester
CSE	cottonseed methyl ester
DC	discrete component
E#	#% ethanol/gasoline fraction
FAME	fatty acid methyl ester
HME1	hempseed methyl ester (Ukrainian oil production)
HME2	hempseed methyl ester (EU standard)
JTR	jatropha methyl ester
LME	lard methyl ester
LNE	linseed methyl ester

LP	length parameter
PD	pure diesel fuel
E0	pure gasoline fuel
PME	palm methyl ester
PMK	palm kernel methyl ester
PTE	peanut methyl ester
RME	rapeseed methyl ester
SFE	safflower methyl ester
SMD	Sauter mean diameter
SME	soybean methyl ester
SNE	sunflower methyl ester
TGE	tung methyl ester
TME	tallow methyl ester
WCO	waste cooking oil
YGR	yellow grease methyl ester

Symbols

A	spray penetration coefficient
d	nozzle diameter [m]
D	diffusion coefficient [$m^2\ s^{-1}$]
k	thermal conductivity [$W\ m^{-1}\ K^{-1}$]
p	pressure [Pa]
T	temperature [K]
R	radius [μm]
t	time [ms]
U	velocity [ms^{-1}]
Y	mass fraction
κ	thermal diffusivity
μ	dynamic viscosity [Pa s]
ρ	density [$kg\ m^{-3}$]

σ	surface tension [N m^{-1}]
v	kinematic viscosity [m^2 s^{-1}]
χ	recirculation coefficient

Subscripts

d	droplet
eff	effective properties
f	fuel
g	gas
i	liquid species
inj	injection
l	liquid
0	initial condition
s	droplet surface

Author details

Mansour Al Qubeissi[1]*, Nawar Al-Esawi[1] and Ruslana Kolodnytska[2]

*Address all correspondence to: mansour.qubeissi@coventry.ac.uk

1 Centre for Mobility and Transport, Faculty of Engineering, Environment and Computing, Coventry University, Coventry, United Kingdom

2 Faculty of Mechanical Engineering, Zhytomyr State Technological University, Zhytomyr, Ukraine

References

[1] Lapuerta M, Rodríguez-Fernández J, Armas O. Correlation for the estimation of the density of fatty acid esters fuels and its implications. A proposed biodiesel Cetane index. Chemistry and Physics of Lipids. 2010;**163**(7):720. DOI: 10.1016/j.chemphyslip.2010.06.004

[2] Meher LC, Vidya Sagar D, Naik SN. Technical aspects of biodiesel production by transesterification—A review. Renewable and Sustainable Energy Reviews. 2006;**10**:248-268. DOI: 10.1016/j.rser.2004.09.002

[3] Pan K-L, Li J-W, Chen C-P, Wang C-H. On droplet combustion of biodiesel fuel mixed with diesel/alkanes in microgravity condition. Combustion and Flame. 2009;**156**:1926-1936. DOI: 10.1016/j.combustflame.2009.07.020

[4] US Department of Energy: Energy Efficiency and Renewable Energy. Biodiesel Blends. 2015. http://www.afdc.energy.gov/fuels/biodiesel_blends.html [Accessed July 29, 2017]

[5] EPA U. US Environmental Protection Agency 2014. http://www.epa.gov/ [Accessed July 29, 2017]

[6] Yuan W, Hansen AC, Zhang Q. Predicting the physical properties of biodiesel for combustion modeling. Transactions of ASAE. 2003;**46**:1487-1493. DOI: 10.13031/2013.15631

[7] Pearson RJ, Turner JWG. Using alternative and renewable liquid fuels to improve the environmental performance of internal combustion engines: Key challenges and blending technologies. Alternative Fuels and Advanced Vehicle Technologies for Improved Environmental Performance, Elsevier. 2014:52-89. DOI: 10.1533/9780857097422.1.52

[8] Brunschwig C, Moussavou W, Blin J. Use of bioethanol for biodiesel production. Progress in Energy and Combustion Science. 2012;**38**:283-301. DOI: 10.1016/j.pecs.2011.11.001

[9] Sazhin SS. Modelling of fuel droplet heating and evaporation: Recent results and unsolved problems. Fuel. 2017;**196**:69-101. DOI: 10.1016/j.fuel.2017.01.048

[10] Al Qubeissi M. Heating and Evaporation of Multi-Component Fuel Droplets. Stuttgart: WiSa; 2015

[11] Samimi Abianeh O, Chen CP. A discrete multicomponent fuel evaporation model with liquid turbulence effects. International Journal of Heat and Mass Transfer. 2012;**55**:6897-6907. DOI: 10.1016/j.ijheatmasstransfer.2012.07.003

[12] Ra Y, Reitz RD. A vaporization model for discrete multi-component fuel sprays. International Journal of Multiphase Flow. 2009;**35**:101-117. DOI: 10.1016/j.ijmultiphaseflow.2008.10.006

[13] Zhu G-S, Reitz RD. A model for high-pressure vaporization of droplets of complex liquid mixtures using continuous thermodynamics. International Journal of Heat and Mass Transfer. 2002;**45**:495-507. DOI: 10.1016/S0017-9310(01)00173-9

[14] Laurent C, Lavergne G, Villedieu P. Continuous thermodynamics for droplet vaporization: Comparison between gamma-PDF model and QMoM. Comptes Rendus Mécanique. 2009;**337**:449-457. DOI: 10.1016/j.crme.2009.06.004

[15] Grote M, Lucka K, Köhne H. Multicomponent Droplet Evaporation of Heating Oil Using a Continuous Thermodynamics Model. Lisbon, Portugal: V ECCOMAS CFD; 2010

[16] Burger M, Schmehl R, Prommersberger K, Schäfer O, Koch R, Wittig S. Droplet evaporation modeling by the distillation curve model: Accounting for kerosene fuel and elevated pressures. International Journal of Heat and Mass Transfer. 2003;**46**:4403-4412. DOI: 10.1016/S0017-9310(03)00286-2

[17] Smith BL, Bruno TJ. Advanced distillation curve measurement with a model predictive temperature controller. International Journal of Thermophysics. 2006;**27**:1419-1434. DOI: 10.1007/s10765-006-0113-7

[18] Qi DH, Lee CF. Influence of soybean biodiesel content on basic properties of biodiesel-diesel blends. Journal of the Taiwan Institute of Chemical Engineers. 2014;**45**:504-507. DOI: 10.1016/j.jtice.2013.06.021

[19] Sazhin SS, Elwardany A, Krutitskii PA, Castanet G, Lemoine F, Sazhina EM, et al. A simplified model for bi-component droplet heating and evaporation. International Journal of Heat and Mass Transfer. 2010;**53**:4495-4505. DOI: 10.1016/j.ijheatmasstransfer.2010.06.044

[20] Elwardany AE, Gusev IG, Castanet G, Lemoine F, Sazhin SS. Mono- and multi-component droplet cooling/heating and evaporation: Comparative analysis of numerical models. Atom Sprays. 2011;**21**:907-931. DOI: 10.1615/AtomizSpr.2012004194

[21] Sazhin SS. Droplets and Sprays. London: Springer; 2014

[22] Al Qubeissi M, Sazhin SS, Elwardany AE. Modelling of blended diesel and biodiesel fuel droplet heating and evaporation. Fuel. 2017;**187**:349-355. DOI: 10.1016/j.fuel.2016.09.060

[23] Al Qubeissi M, Sazhin SS. Blended biodiesel/Diesel fuel droplet heating and evaporation. vol. DHE-01. Brighton, UK. 2016. p. 179

[24] Al Qubeissi M, Al-Esawi N, Sazhin SS. Droplets heating and evaporation: An application to diesel-biodiesel fuel mixtures. Universitat Politècnica València. 2017. DOI: 10.4995/ILASS2017.2017.4644

[25] Al Qubeissi M, Sazhin S, Al-Esawi N. Models for automotive fuel droplets heating and evaporation. Universitat Politècnica València. 2017. DOI: 10.4995/ILASS2017.2017.4754

[26] Sazhin SS, Al Qubeissi M, Kolodnytska R, Elwardany AE, Nasiri R, Heikal MR. Modelling of biodiesel fuel droplet heating and evaporation. Fuel. 2014;**115**:559-572. DOI: 10.1016/j.fuel.2013.07.031

[27] Al Qubeissi M, Sazhin SS, Turner J, Begg S, Crua C, Heikal MR. Modelling of gasoline fuel droplets heating and evaporation. Fuel. 2015;**159**:373-384. DOI: 10.1016/j.fuel.2015.06.028

[28] Sazhin SS, Al Qubeissi M, Nasiri R, Gun'ko VM, Elwardany AE, Lemoine F, et al. A multi-dimensional quasi-discrete model for the analysis of diesel fuel droplet heating and evaporation. Fuel. 2014;**129**:238-266. DOI: 10.1016/j.fuel.2014.03.028

[29] Kolodnytska R, Al Qubeissi M, Sazhin SS. Biodiesel fuel droplets: Transport and thermodynamic properties. 25th Eur. Conf. Liq. Atom. Spray Syst., vol. No. 7 (CD), Crete, Greece: 2013

[30] Elwardany AE. Modelling of multi-component fuel droplets heating and evaporation. PhD thesis. University of Brighton, 2012

[31] Eggers J. Breakup and Coalescence of Free Surface Flows. Handb. Mater. Model. 1st ed., Netherlands: Springer; 2005, p. 1403-1416

[32] Kolodnytska R. LP-model for Biodiesel Spray Penetration. Annu. Conf. Liq. Atom. Spray Syst., Brighton, UK: University of Brighton; 2016, p. 105-106

[33] Chen L, Liu Z, Sun P, Huo W. Formulation of a fuel spray SMD model at atmospheric pressure using design of experiments (DoE). Fuel. 2015;**153**:355-360. DOI: 10.1016/j.fuel.2015.03.013

[34] Grabar IG, Kolodnytska RV, Semenov VG. Biofuel Based on Oil for Diesel Engines. ZDTU: Zhytomyr; 2011

[35] Sazhin SS. Advanced models of fuel droplet heating and evaporation. Progress in Energy and Combustion Science. 2006;**32**:162-214. DOI: 10.1016/j.pecs.2005.11.001

[36] Al Qubeissi M, Sazhin SS, Crua C, Turner J, Heikal MR. Modelling of biodiesel fuel droplet heating and evaporation: Effects of fuel composition. Fuel. 2015;**154**:308-318. DOI: 10.1016/j.fuel.2015.03.051

[37] De Cock N, Massinon M, Salah SOT, Lebeau F. Investigation on optimal spray properties for ground based agricultural applications using deposition and retention models. Biosystems Engineering. 2017;**162**:99-111. DOI: 10.1016/j.biosystemseng.2017.08.001

[38] Ranade S, Bajaj A, Londhe V, Babul N, Kao D. Fabrication of topical metered dose film forming sprays for pain management. European Journal of Pharmaceutical Sciences. 2017;**100**:132-141. DOI: 10.1016/j.ejps.2017.01.004

[39] Abramzon B, Sirignano WA. Droplet vaporization model for spray combustion calculations. International Journal of Heat and Mass Transfer. 1989;**32**:1605-1618. DOI: 10.1016/0017-9310(89)90043-4

[40] Crua C, Heikal MR, Gold MR. Microscopic imaging of the initial stage of diesel spray formation. Fuel. 2015;**157**:140-150. DOI: 10.1016/j.fuel.2015.04.041

[41] Eggers J, Villermaux E. Physics of liquid jets. Reports on Progress in Physics. 2008; **71**:036601. DOI: 10.1088/0034-4885/71/3/036601

[42] Crua C, de Sercey G, Gold M, Heikal MR. Image-based analysis of evaporating diesel sprays in the near-nozzle region. 25th Eur. Conf. Liq. Atom. Spray Syst., Chania, Greece: 2013

[43] Kolodnytska R, Skurativskyi S, Moskvin. Maximum Entropy Method for Biodiesel Spray Droplet Distribution. Valencia, Spain: Universitat Politècnica València: Polytech. Univ. Valencia Congr. ILASS2017; 2017. DOI: 10.4995/ILASS2017.2017.4769

[44] Crua C, de Sercey G, Heikal MR, Gold M. Dropsizing of Near-Nozzle Diesel and RME Sprays by Microscopic Imaging. ICLASS 2012, Heidelberg, Germany: 2012